https://doi.org/10.5194/egusphere-2023-2319
Preprint. Discussion started: 9 November 2023

Prominent role of organics in aerosol liquid water content over the south-eastern Atlantic during biomass burning season

Lu Zhang[1,2], Michal Segal-Rozenhaimer[1,3,4], Haochi Che[1,2], Caroline Dang[3,4], Junying Sun[5], Ye Kuang[6,7], Paola Formenti[8]

[1]Department of Geophysics, Porter School of the Environment and Earth Sciences, Tel Aviv University, Tel Aviv, Israel

[2]Department of Geosciences, University of Oslo, Oslo, Norway

[3]Bay Area Environmental Research Institute, Moffett Field, California, USA

[4]NASA Ames Research Center, Moffett Field, California, USA

[5]State Key Laboratory of Severe Weather & Key Laboratory of Atmospheric Chemistry, Chinese Academy of Meteorological Sciences, Beijing, China

[6]Institute for Environmental and Climate Research, Jinan University, Guangzhou, China

[7]Guangdong-Hongkong-Macau Joint Laboratory of Collaborative Innovation for Environmental Quality, Guangzhou, China

[8]Université Paris Cité and Univ Paris Est Creteil, CNRS, LISA, Paris, France

Correspondence: Michal Segal-Rozenhaimer (msegalro@tauex.tau.ac.il) and Haochi Che (haochi.che@geo.uio.no)

https://doi.org/10.5194/egusphere-2023-2319
Preprint. Discussion started: 9 November 2023

Abstract

The interaction between atmospheric aerosols and moisture is crucial for aerosol properties and their climate effects. In this study, thanks to the rich measurements of aerosol properties during the 2016 and 2018 ORACLES campaigns, we investigate the aerosol liquid water content (ALWC) over the south-eastern Atlantic Ocean during the biomass burning (BB) season, as well as the seldom-reported ALWC associated with organic aerosols (OA) ($ALWC_{OA}$) (OA). $ALWC_{OA}$ is determined using the OA hygroscopicity parameter κ_{OA}, derived from in-situ hygroscopicity measurements, particle number size distribution, and chemical composition. The ALWC can be determined either with the overall hygroscopic parameter $\kappa_{f(RH)}$ or from the sum of $ALWC_{OA}$ and the ALWC simulated from ISORROPIA-II, a thermodynamic equilibrium model for inorganic aerosol. The ALWC from both methods is highly correlated at all RHs with an R^2 of 0.99. The ALWC increases with aerosol loading and ambient relative humidity (RH). Due to the lower RH and higher aerosol loading in the 2016 campaign, the ALWC for both campaigns are generally consistent. $ALWC_{OA}$ accounts for 38±16 % of the total ALWC during both campaigns. Notably, the contribution of $ALWC_{OA}$ is greater than commonly reported in the literature, highlighting the significance of OA in ALWC and therefore the aerosol direct radiative forcing in this climatically significant region. The strong correlation between κ_{OA} and $ALWC_{OA}/ALWC$, as indicated by an R^2 value of 0.72, underscores the importance of a good estimation of κ_{OA} in the ALWC estimation. Additionally, the significant difference between $ALWC_{OA}$ values calculated using real-time κ_{OA} and those calculated with the campaign mean κ_{OA}, highlights the limitation of using a constant κ_{OA} value, a practice commonly adopted in climate models.

Keywords: hygroscopicity, κ_{OA}, liquid water content, biomass burning, organic aerosol, Atlantic, airborne measurements

https://doi.org/10.5194/egusphere-2023-2319
Preprint. Discussion started: 9 November 2023

1 Introduction

Wildfires and open burning emit ~34–41 Tg yr^{-1} of biomass burning aerosol (BBA) to the atmosphere (Schill et al., 2020), with ~ 1/3 coming from Africa, a region where the burned area is increasing every year (van der Werf et al., 2010; Andela et al., 2017). Each austral spring, BBA particles from African fires travel westward through the free troposphere (FT) over the stratocumulus cloud deck in the south-eastern Atlantic (SEA). Accompanied by moisture within these plumes, BBAs interact with the moisture and exert significant impacts on regional radiation and climate (Redemann et al., 2021; Pistone et al., 2021; Adebiyi et al., 2015).

Aerosol liquid water (ALW), resulting from aerosol-moisture interactions, is the most abundant species in the particle phase and plays a crucial role in various atmospheric chemical and physical processes. ALW affects aerosol optical properties and radiative effects, especially for relative humidity (RH) > 60% (Burgos et al., 2019; Kuang et al., 2018; Zhang et al., 2015). It is considered to be the major contributor to aerosol direct radiative cooling (Pilinis et al., 1995). Additionally, ALW serves as a medium for chemical reactions, facilitating the formation of secondary aerosols (Kuang et al., 2020c; Song et al., 2019; Wang et al., 2016).

However, despite its widespread presence and critical role, the content and distribution of ALW are not well documented in the literature due to technological limitations that direct measurement is not attainable (Kuang et al., 2018). Current methodologies primarily rely on indirect estimates of aerosol liquid water content (ALWC) either from thermal equilibrium models (Jin et al., 2020; Guo et al., 2015) or aerosol hygroscopicity measurements (Kuang et al., 2018). Although the ALWC of inorganics can now be well simulated with thermal equilibrium models such as the ISORROPIA II thermodynamic model (Nenes et al., 1998) or the Aerosol Inorganics Model (Wexler and Clegg, 2002), the situation becomes particularly complex when attempting to quantify the ALWC associated with organic aerosol (OA).

https://doi.org/10.5194/egusphere-2023-2319
Preprint. Discussion started: 9 November 2023

The ALWC associated with OA is typically calculated using the hygroscopicity of OA, termed κ_{OA} (Petters and Kreidenweis, 2007). However, due to the chemical complexity of atmospheric OA, κ_{OA} remains poorly characterised (Kuang et al., 2020a). Studies have employed regression between κ and OA fraction to calculate κ_{OA} for its simplicity (Che et al., 2016; Pöhlker et al., 2023); however, this method assumes a constant κ for OA during calculation, which could greatly underestimate the variation of κ_{OA}. In fact, κ_{OA} values can fluctuate considerably, from 0 for hydrophobic, freshly emitted organics, to over 1.0 for highly hygroscopic amino acids (Zhang et al., 2007; Petters et al., 2009). Even within a single site, κ_{OA} can show a distinct diurnal variation (Deng et al., 2019; Kuang et al., 2020b). Existing empirical parameterisations, mainly between κ_{OA} and the OA oxidation level, typically characterised by the oxygen-to-carbon (O/C) ratio or the fraction of total organic mass spectral signal at m/z 44 (f_{44}) (Lambe et al., 2011; Mei et al., 2013) from field experiments, have attempted to address this variability. However, these parameterisations can vary spatially and temporally and are not always well constrained (Kuang et al., 2020a; Cerully et al., 2015; Rickards et al., 2013). Moreover, some researchers apply κ_{OA} values or their parameterisations obtained from supersaturation conditions, such as measurements of cloud condensation nuclei, to estimate ALWC. This approach could lead to overestimations, as κ_{OA} values from supersaturated conditions could be higher than those obtained at sub-saturated conditions (Rastak et al., 2017; Guo et al., 2015; Petters and Kreidenweis, 2007). Hygroscopicity measurements from techniques such as humidified tandem differential mobility analyser or humidified nephelometer under sub-saturated conditions are more suitable for ALWC calculations.

The ORACLES (ObseRvations of Aerosols above CLouds and their intEractionS) campaign (Redemann et al., 2021) presents a comprehensive observation of BBAs from African fires, including aerosol hygroscopicity measurements, enabling the in-depth

https://doi.org/10.5194/egusphere-2023-2319
Preprint. Discussion started: 9 November 2023

investigation of the rare-reported vertical profiles of ALWC from aerosols and those associated with OA over the SEA. Our findings are expected to enhance the current treatment of hygroscopicity and ALWC and those of OA in climate models and satellite retrievals, thereby enriching the understanding of aerosol-cloud-interactions and radiative assessments in this climatically crucial SEA region.

2 Methods

2.1 Aircraft Instrumentation and Data Analysis

We analyse in situ airborne data measured over the SEA region from the ORACLES 2016 and 2018 campaign (Redemann et al., 2021). The ORACLES 2016 and 2018 campaign took place from 31st August to 24th September and from 30th September to 21st October 2018, respectively. All instruments were mounted on the NASA P-3 aircraft. The scattering enhancement factor, f(RH), was measured by two Radiance Research M903 integrating nephelometers (Nephs) operated in parallel, one under relatively dry conditions and the other at around 80 % RH. The uncertainty of f(RH) was estimated to be ~ 20 % for RH < 85 % (Titos et al., 2016; Zieger et al., 2013). Scattering coefficients and f(RH) are reported at 540 nm wavelength. Non-refractory submicron aerosol compositions were measured by a High-Resolution Time-of-Flight Aerosol Mass Spectrometer (HR-ToF-AMS, Aerodyne Research Inc.) and the refractory BC was determined by a single particle soot photometer (SP2, Droplet Measurement Technology). The particle number size distribution (PNSD) was from an ultra-high-sensitivity aerosol spectrometer (UHSAS) and an aerodynamic particle sizer (APS). The aerosol/plume age was simulated with a two-week forecast utilizing the Weather Research and Aerosol Aware Microphysics (WRF-AAM) model (Thompson and Eidhammer, 2014). All measurements were averaged over 15 s and adjusted to STP values at 273.15 K and 1013 hPa. The ALWC has only been calculated when temperature > 0 °C. Measurements from 21 flights,

https://doi.org/10.5194/egusphere-2023-2319
Preprint. Discussion started: 9 November 2023

totalling approximately 134 flight hours, were analysed in this study. For more information on instrumentation and data quality control, refer to Zhang et al. (2023).

2.2 Calculation of *f*(RH)

The aerosol scattering enhancement factor, *f*(RH), is calculated as:

$$f(RH) = \frac{\sigma_{sp}(RH)}{\sigma_{sp}\left(RH_{dry}\right)}, \quad (1)$$

where $\sigma_{sp}(RH)$ and $\sigma_{sp}(RH_{dry})$ represent the scattering coefficients at humidified and dry RHs (RH and RH_{dry}), respectively. Previous studies usually take RH_{dry} as 30-40 % assuming aerosols are dry at/under such RHs (Burgos et al., 2019; WMO/GAW, 2016; Titos et al., 2016). In this study, to facilitate comparison with previous studies and minimize the influence of water, we only included the *f*(RH) with RH_{ref} equal to or smaller than 30 %.

2.3 Calculation of ALWC

In this study, we calculate ALWC utilizing two methods. The first employs $\kappa_{f(RH)}$, the aerosol hygroscopicity parameter κ retrieved from *f*(RH) (Zieger et al., 2010). It can be considered as the scattering coefficient weighted average κ (Kuang et al., 2021). The detailed procedure of $\kappa_{f(RH)}$ retrieval can be found in Zhang et al. (2023). In Section 3.3 of Kuang et al. (2020b), the authors meticulously demonstrated that $\kappa_{f(RH)}$ can accurately represent the κ_{chem} of PM_1 (particulate matter with an aerodynamic diameter less than 1 μm). By substituting κ_{chem} with $\kappa_{f(RH)}$, the aerosol liquid water content, ALWC, can be calculated with the equation below (Petters and Kreidenweis (2007), Eq. 5):

$$\mathrm{ALWC}_{\kappa_{f(RH)}} = \frac{a_w}{1 - a_w} \cdot V_{p,dry} \cdot \kappa_{f(RH)} \cdot \rho_w \quad (2)$$

where a_w is the water activity, which can be replaced by RH ignoring the curvature effect for particles with diameter larger than 100 nm. $V_{p,dry}$ represents the dry particle volume, calculated as the sum of the volumes of inorganics, OA, and BC under dry conditions. The volumes of

https://doi.org/10.5194/egusphere-2023-2319
Preprint. Discussion started: 9 November 2023

inorganics are calculated according to the modified ion-pairing scheme of Zhang et al. (2022). The volumes of OA and BC are converted from the mass of OA from AMS and that of BC from SP2. The densities of the inorganics, OA, and BC are given in Table S1 in Zhang et al. (2023). ρ_w is water density, taken as 1 g cm^{-3}.

ALWC can also be calculated as the sum of that related to inorganics and organics. The water associated with inorganic species ($ALWC_{inorg}$) can be predicted with ISORROPIA-II, which is an aerosol thermodynamic model that calculates the concentration of inorganic species that exist in the gas and aerosol phase at chemical equilibrium (Fountoukis and Nenes, 2007; Nenes et al., 1998). ISORROPIA-II has been widely used in atmospheric research (e.g. Guo et al., 2015) and has been implemented in several models, such as GEOS-Chem (http://wiki.seas.harvard.edu/geos-chem/index.php/ISORROPIA_II) and EMAC chemistry climate model (Milousis et al., 2023). Input variables include inorganic ions from AMS and the ambient RH and temperature. ISORROPIA-II can address two states, the stable state, which assumes the coexistence of liquid aerosol and solid crystalline salts, and metastable state, assuming all aerosols are in the liquid phase. BBAs from African fires are accompanied by large amounts of moisture (Fig. 1, Pistone et al., 2021), and as they are transported in the free troposphere, their RH decreases. Many key atmospheric compounds, such as $(NH_4)_2SO_4$ and NH_4NO_3, exhibit lower ERH (efflorescence relative humidity) than deliquescence RH, DRH (Peng et al., 2022). Therefore, we assume the aerosols in our study primarily reside on the upper metastable branch of the hygroscopic hysteresis curve, leading to the application of the metastable state in ISORROPIA-II. The limitation of this assumption and the uncertainty of ISORROPIA-II under low RH are discussed in Sect. 3.3. The sum of $ALWC_{inorg}$ and the dry mass of inorganics can be regarded as the mass of inorganics under ambient conditions, $Mass_{Inorg,ambient}$.

https://doi.org/10.5194/egusphere-2023-2319
Preprint. Discussion started: 9 November 2023

The water associated with organics, $ALWC_{OA}$, was calculated using the following equation (Petters and Kreidenweis, 2007):

$$ALWC_{OA} = \frac{a_w}{1 - a_w} \cdot \frac{m_{OA}}{\rho_{OA}} \cdot \kappa_{OA} \cdot \rho_w \quad (3)$$

where κ_{OA} represents the hygroscopicity parameter of OA. Its calculation is referred to Zhang et al. (2023). It is worthnoting that the κ_{OA} is the bulk κ of OA in PM_1. m_{OA} and ρ_{OA} represent the organic mass from AMS and the density of OA. The sum of m_{OA} and $ALWC_{OA}$ can be considered as the mass of OA under ambient conditions, $Mass_{OA,ambient}$. The sum of $Mass_{Inorg,ambient}$, $Mass_{OA,ambient}$, and BC mass from SP2 can be regarded as the mass of PM_1 under ambient conditions, $Mass_{PM1,ambient}$. The ALWC can also be calculated as the sum of $ALWC_{OA}$ and $ALWC_{inorg}$, denoted $ALWC_{OA+ISRP}$,

$$ALWC_{OA+ISRP} = ALWC_{inorg} + ALWC_{OA}. \quad (4)$$

The agreement between ALWC calculated from the two methods, namely $ALWC_{\kappa_{f(RH)}}$ and $ALWC_{OA+ISRP}$, is evaluated in Section 3.3.

3 Result and discussion

3.1 Overview of meteorology

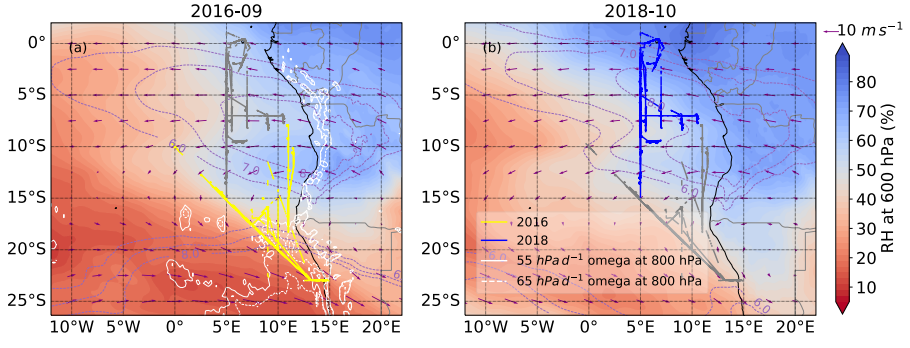

https://doi.org/10.5194/egusphere-2023-2319
Preprint. Discussion started: 9 November 2023

Figure 1. Maps of the (a) September mean and (b) October mean of ERA5 600 hPa RH overlaid by the 600 hPa zonal wind (purple contours; 6, 7, and 8 m s^{-1}), 600 hPa horizontal wind vector (purple arrows; m s^{-1}), and ORACLES flight tracks in 2016 (yellow) and 2018 (blue), respectively. White contours in (a) are the 2016 September mean vertical velocity, omega, at 800 hPa. Solid and dashed lines represent the subsidence of 55 and 65 hectopascals per day (hPa d^{-1}), respectively. Flight tracks in grey are drawn for reference.

This section gives an overview of the meteorology of the detected regions in 2016 and 2018 ORACLES campaign. Figure 1 shows the flight tracks with 600 hPa RH and zonal and horizontal wind from European Center for Medium-Range Weather Forecasts reanalysis v5 (ERA5) in September 2016 and October 2018. These two months were chosen as most flights fall within this period. As shown in Fig. 1, the southern African Easterly Jet (AEJ-S) is one of the most important characteristic features in the SEA; it is defined as the zonal easterlies centered at 8° S around 600 -700 hPa with speed exceeding 6 m s^{-1} and is a good carrier of aerosols and accompanied moisture from the BB in Africa (Adebiyi and Zuidema, 2016). Studies show that ~55 % of the BBAs emitted from African fires are transported westward over the SEA with the AEJ-S (Adebiyi and Zuidema, 2016). Another characteristic circulation is the African continent mid-level (~600 hPa) anticyclone (Fig. 1), to the south of the AEJ-S, aerosols recirculated by which would transport southward, merge with mid-latitude westerly winds and eventually return to the African continent at around 18° S (Ryoo et al., 2021). At a similar altitude (20-25° S), around 10° E at 925-950 hPa, there is the Benguela low-level jet (LLJ) (Nicholson, 2010). It is located off the coast of Namibia and the subsidence (Fig. 1a) it generates is expected to facilitate the entrainment of aerosols into the marine boundary layer (MBL) (Redemann et al., 2021; Ryoo et al., 2021).

Flights in ORACLES 2018 (Fig. 1b, blue lines) are in the region of 0-15° S and 5-10° E, generally within the coordinates where the AEJ-S lies. The plumes emitted by African fires,

https://doi.org/10.5194/egusphere-2023-2319
Preprint. Discussion started: 9 November 2023

which are lifted in the convective boundary layer up to ~6 km in the free troposphere (FT), are directly transported westwards from the continent by the AEJ-S (Fig. S1). These aerosols then interact with one of the Earth's largest subtropical stratocumulus cloud decks and subside into the MBL (Redemann et al., 2021; Che et al., 2022). Therefore, in the 2018 ORACLES campaign, aerosols generally exhibit higher loading, higher RH, and less aging at higher altitudes. Conversely, as altitude decreases, aerosol concentration and RH (above MBL) decrease while their age increases (Fig. 2 and Fig. S2). In contrast to the 2018 campaign, most of the flight tracks in ORACLES 2016 are more southerly (Fig. 1a and Fig. S1a, yellow lines) and the circulation is more complicated. At mid-level, flights pass through both the AEJ-S region and the continent anticyclone, encountering both less aged aerosols coming directly from the continent and highly aged aerosols transported all the way from the west/north. Those aerosols transported over long distances generally show smaller loading and lower RH. At lower altitudes, aerosols can be less aged than those in 2018 at similar longitudes due to the subsidence near the Namibian coast (Fig. 1a). Since September 2016 has a much weaker plume than October 2018 (Redemann et al., 2021, e.g. Fig. 9), the 2016 flights generally encounter higher aerosol loadings and lower RH than 2018 campaign, aged aerosols were detected in both campaigns with a plume age of 7.2±2.6 d and $f44$ of 0.21±0.03 (Fig. 1, S2, and 2).

https://doi.org/10.5194/egusphere-2023-2319
Preprint. Discussion started: 9 November 2023

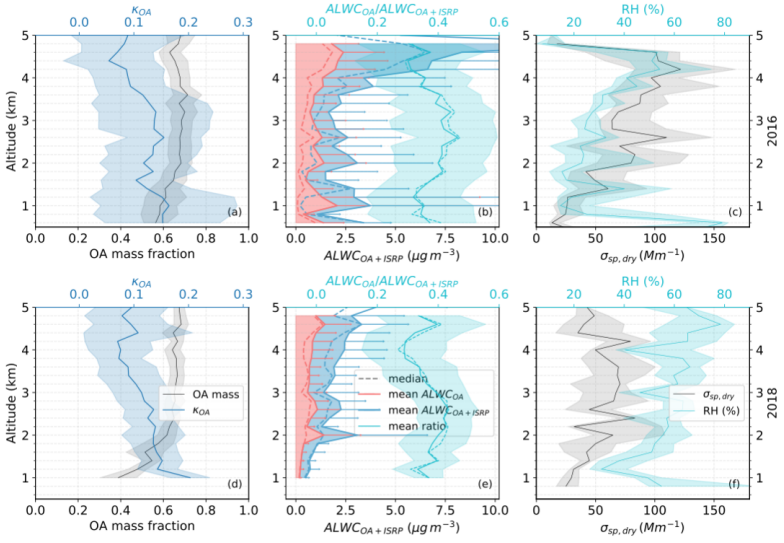

Figure 2. The vertical distribution of various aerosol properties. (a, d) Vertical distributions of OA mass fraction (grey) and κ_{OA} (cyan) in 2016 and 2018 ORACLES campaigns, respectively. The lines and shades represent the average and standard deviation in every 200 m bin, respectively. (b, e) Vertical distribution of aerosol liquid water content associated with OA, $ALWC_{OA}$ (red), the $ALWC_{OA+ISRP}$ (blue), calculated as the sum of $ALWC_{OA}$ and $ALWC_{inorg}$ from ISORROPIA-II model, and the fraction of $ALWC_{OA}$ in $ALWC_{OA+ISRP}$ in 2016 (b) and 2018 (e) ORACLES campaigns, respectively. The solid and dashed lines represent the mean and median in every 200 m bin, respectively. Error bars and shades represent 1 standard deviation. (c, f) Vertical variation of dry scattering coefficient, $\sigma_{sp,dry}$ (grey) and RH (cyan) in 2016 (c) and 2018 (f) ORACLES campaigns, respectively. The lines and shades represent the average and standard deviation in every 200 m bin, respectively.

3.2 The hygroscopicity of OA in SEA during BB season

https://doi.org/10.5194/egusphere-2023-2319
Preprint. Discussion started: 9 November 2023

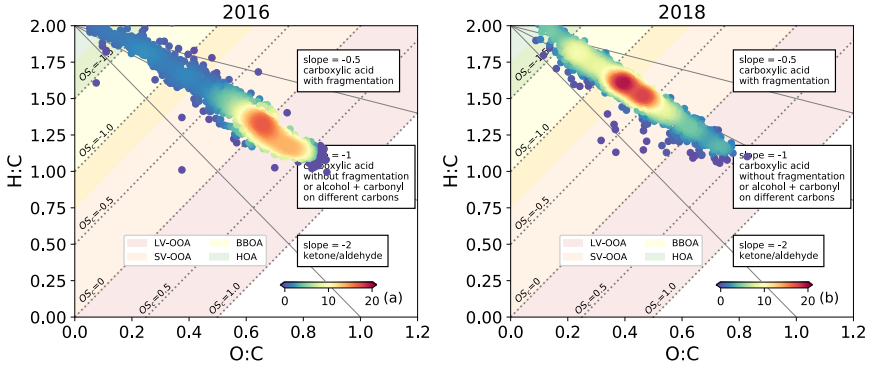

Figure 3. Van Krevelen diagrams (H/C vs. O/C) for 2016 (a) and 2018 (b) ORACLES campaign. The color scale indicates the density of the data in each plot. The estimated carbon oxidation states (OS_C=2O/C−H/C) are shown with the dotted lines. Slope descriptions are from Ng et al. (2011).

The hygroscopicity of OA is a key parameter in the calculation of the ALWC associated with OA and is therefore crucial in assessing the significance of OA in ALWC. We first analyzed the characteristics of OA over SEA during the BB season. The slope of the Van Krevelen diagram is around -1 in both years (Fig. 3), resembling the addition of carboxylic acid groups to aerosols as they age. The OSc concentrates around 0.1 for 2016 and -0.7 for 2018, indicating that the majority of the OA belongs to LV-OOA in 2016 and SV-OOA in 2018. The high f_{44} values, 0.21±0.03 for 2016 and 0.21±0.02 for 2018 (Fig. S2), are consistent with the highly oxidized BBOA in CLARIFY (Wu et al., 2020). The relatively low OS_C and high f_{44} reflect the highly oxidized and semi-volatile to low volatility nature of OA in ORACLES. This is compatible with the findings from Dang et al. (2022) that higher-volatility OA appears to be associated with more aged BB plumes and Dobracki et al. (2022) and Zhang et al. (2023) that fragmentation plays a vital role in OA loss during the transport in the SEA.

The κ_{OA} value ranges from 0.00 (5th percentile) to 0.23 (95th percentile) with the 25th and 75th percentiles of 0.06 and 0.16, respectively. This substantial variation might result from

https://doi.org/10.5194/egusphere-2023-2319
Preprint. Discussion started: 9 November 2023

the large variations of the aging days of aerosols during transport. The average κ_{OA} is 0.11±0.08, which is at the upper median level compared to the results from laboratory and field studies (Kuang et al., 2020b; Rastak et al., 2017; Mei et al., 2013; Engelhart et al., 2011; Lambe et al., 2011). The 5 % negative κ_{OA} might be caused by the uncertainty in the calculation. It might be also partly contributed by phase-separated particles with organic shells and inorganic cores in ORACLES. Specifically, the organic shell can act as a barrier for water vapour exchange with the inorganic core and increase the DRH of the inorganics (Li et al., 2021). At high RH, e.g. >94%, it does not affect κ much; while at lower RH, such as 80 %, the inorganics may not be fully deliquescent, causing the κ for inorganics calculated with the ZSR mixing rule to be overestimated and eventually results in a negative κ_{OA}. However, such particles with organic shell are rare from our TEM analysis performed for ORACLES (Dang et al., 2021).

The vertical distribution of κ_{OA} are similar to those of f(80%) and $\kappa_{f(RH)}$, with higher values at low altitude (Fig. 2a). This trend is also similar to that of $f44$ and plume age (Fig. S2), especially in 2018. Many studies have found significant positive correlations between κ_{OA} and OA oxidation level in terms of f_{44} or O/C (Kuang et al., 2020b; Lambe et al., 2011; Mei et al., 2013). Although the vertical trends of κ_{OA} and plume age or f_{44} seem to be correlated (Fig. 2 and S2), no clear relationship was found in this study between κ_{OA} and OA oxidation level, with a Pearson correlation coefficient of 0.14 with the plume age and 0.04 with f_{44}. This underscores the limitations of the relationship between κ_{OA} and the OA oxidation level and calls for caution when applying this relationship to atmospheric studies.

3.3 Aerosol liquid water content (ALWC)

3.3.1 Vertical distribution of aerosol liquid water content (ALWC)

https://doi.org/10.5194/egusphere-2023-2319
Preprint. Discussion started: 9 November 2023

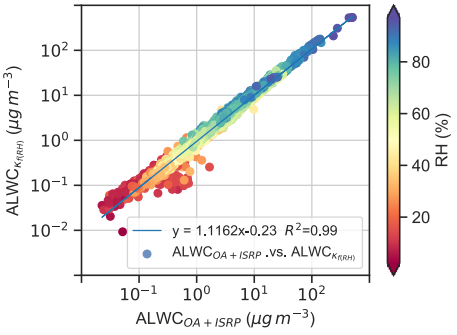

Figure 4. Comparison of ALWC calculated from f(RH) , ALWC$_{\kappa_{f(RH)}}$, and ALWC$_{OA+ISRP}$, the sum of ALWC$_{inorg}$ (water associated with inorganics from ISOPPROPIA-II) and ALWC$_{OA}$ (water associated with OA).

In this section, we investigate the vertical distribution of aerosols and OA. First, we compare the ALWC obtained from aforementioned two methods, ALWC$_{\kappa_{f(RH)}}$, calculated from $\kappa_{f(RH)}$, and ALWC$_{OA+ISRP}$, which is the sum of ALWC$_{inorg}$ from ISOPPROPIA-II and ALWC$_{OA}$ calculated from κ_{OA}. Both methods regard BC as hydrophobic and assume aerosols to stay in the metastable state. Figure 4a illustrates the comparison of ALWC$_{\kappa_{f(RH)}}$ and ALWC$_{OA+ISRP}$; good agreement has been achieved, evidenced by a slope of 1.11 and an R^2 of 0.99. The higher ALWC$_{\kappa_{f(RH)}}$ values might be caused by the different treatment of the mixing state. The ALWC$_{\kappa_{f(RH)}}$ represents the ALWC under the assumption of internal mixing of aerosol particles, as $\kappa_{f(RH)}$ was derived based on internal mixing assumption. Conversely, the ALWC$_{OA+ISRP}$ treats BC independently and serves as an estimate of the ALWC under the external mixing assumption. In addition, the ALWC$_{OA+ISRP}$ considers the ALW associated with inorganics and OA separately.

We acknowledge that the metastable state used in this study might not be representative for all aerosols. Background aerosols and those under extremely low RHs might still remain solid; however, their concentrations are limited and would only lead to a slight overestimation

https://doi.org/10.5194/egusphere-2023-2319
Preprint. Discussion started: 9 November 2023

of ALWC. In addition, it is challenging to determine the portion of solid compounds with the available campaign measurements. Therefore, while the assumption of metastable state could lead to a slight overestimation, mainly at low RHs, it remains our best approach given our current measurements. Besides, the lack of measurements of size-resolved and RH-resolved κ would also lead to small uncertainties, resulting in a small deviation of the calculation of $ALWC_{OA}$. In the following discussion, ALWC is represented by $ALWC_{OA+ISRP}$ unless noted otherwise.

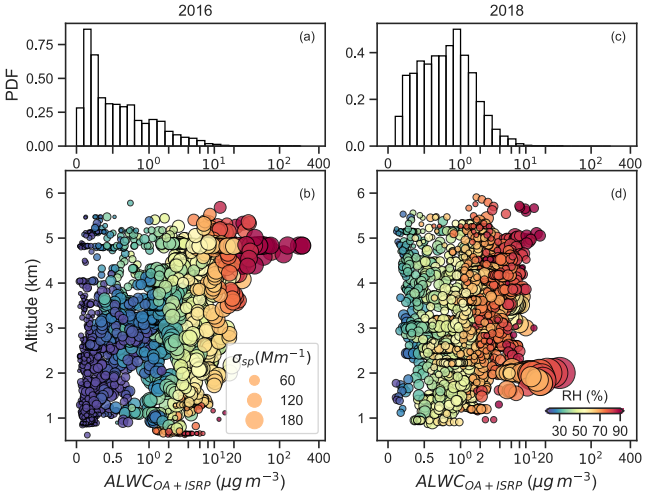

Figure 5. PDF of ALWC in 2016 (a) and 2018 (c) ORACLES campaign. Vertical distributions of ALWC in the 2016 (b) and 2018 (d) ORACLES campaign, coloured by RH and marker size changes with the dry scattering coefficient.

Figure 2b and 5 illustrate the vertical distribution of ALWC in 2016 and 2018 ORACLES campaigns. Figure. 2 shows the vertical distribution of the mean and median values of ALWC, which are mostly smaller than 2.5 μg m^{-3}. The average and median ALWC are 4.4±11.1 μg m^{-3} and 1.6 μg m^{-3} in 2016, respectively, and 2.1±2.0 μg m^{-3} and 1.4 μg m^{-3} in 2018, respectively. The large standard variation and larger mean than median are caused by the

https://doi.org/10.5194/egusphere-2023-2319
Preprint. Discussion started: 9 November 2023

extremely large ALWC values in both campaigns, as evidenced in Fig. 5. From the PDF of ALWC, we found that a fraction of approximately 25 % of the ALWC in 2016 ORACLES is smaller than 0.5 μg m^{-3}, mainly due to the low ambient RH in the flight region (Fig. 1a, Fig. 2c, and more cool-colour circles in Fig. 5b), i.e. 38 % of the RH is lower than 30 % (Fig. 5a and b). In contrast, for 2018 ORACLES, although the aerosol loading was lower (Fig. 2f and smaller markers in Fig. 5d), i.e. an average of 57±37 Mm^{-1} compared to 85±47 Mm^{-1} in 2016, more than half (51 %) of the ALWC is in the range of 0.5-2.0 μg m^{-3} due to the high RH, as shown in Fig. 2f and more warm-colour circles in Fig. 5d. In general, the ALWC over SEA during the BB season are smaller than those obtained over the continent (Ren et al., 2021; Bougiatioti et al., 2016; Wang et al., 2016; Guo et al., 2015) and even several orders of magnitude smaller than in polluted regions (Kuang et al., 2018; Bian et al., 2014). We observed a positive correlation between relative humidity (RH) and ALWC with a Pearson correlation coefficient of 0.7. Aerosol dry scattering coefficient show a much less positive correlation with a Pearson correlation coefficient of 0.3. With the large variation of RH and aerosol loading in this study, aerosol hygroscopicity turns out to be a less significant factor in ALWC, with a Pearson correlation coefficient of 0.1, which is consistent with previous studies (e.g. Guo et al., 2015).

3.3.2 ALWC under various RHs over SEA

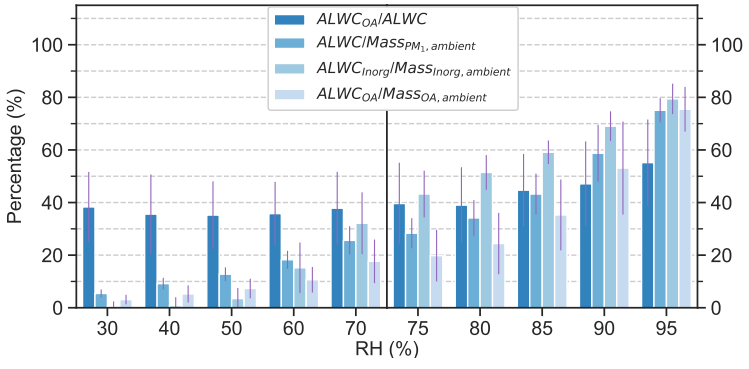

https://doi.org/10.5194/egusphere-2023-2319
Preprint. Discussion started: 9 November 2023

Figure 6. The contribution of $ALWC_{OA}$ to the total ALWC (dark blue bars), the mass fraction of ALWC in ambient aerosol mass (medium-dark blue bars), the fraction of inorganic-related $ALWC_{Inorg}$ in ambient inorganic mass (medium-light blue bars), and the mass fraction of OA-related water $ALWC_{OA}$ in ambient OA mass (very light blue bars) in the 2016 and 2018 ORACLES campaigns. Error bars are 1 standard deviation.

The contribution of $ALWC_{OA}$ to the total ALWC is shown in Fig. 6. Also shown are the mass fraction of water in ambient particles ($ALWC/Mass_{PM1,ambient}$), inorganic-related ALWC in ambient inorganics ($ALWC_{Inorg}/Mass_{Inorg,ambient}$), and OA-associated ALWC in ambient OA ($ALWC_{OA}/Mass_{OA,ambient}$). These variables all increase greatly and monotonically with RH, and reach around 35 %, 50 %, and 25 % at 80 % RH, suggesting water constitutes 35 %, 50 %, and 25 % of OA, inorganics, and particles under 80 % RH, respectively. At 90 % RH, the mass of water taken up exceeds that of the dry particle. Conversely, the variation of the contribution of $ALWC_{OA}$ to the total ALWC ($ALWC_{OA}/ALWC$) is much smaller. It remains stable at around 35% when RH is below 70 %, indicating the increase in OA-associated water is similar to that of inorganic-associated water. Then the contribution of $ALWC_{OA}$ increases monotonically and reaches around 55 % at 95 % RH. This implies that the increase in OA-associated water surpasses the increase in inorganic-associated water as RH increases beyond 70 %. In contrast, the variation of $ALWC_{OA}/ALWC$ with RH in Jin et al. (2020) shows the opposite trend, i.e. higher under low RHs. This is primarily caused by the different assumptions of the compound state. As discussed above, the assumption of metastable state in our study might overestimate the inorganic-associated water and thus underestimate the contribution of $ALWC_{OA}$ to a mild degree, particularly at lower RH conditions. However, Jin et al. (2020) assumed a stable state, with which the ISORROPIA-II algorithm starts with assuming a completely dry particle and as RH increases, dissolves each salt depending on its DRH (Fountoukis and Nenes, 2007). While those particles that are below their DRH and are

https://doi.org/10.5194/egusphere-2023-2319
Preprint. Discussion started: 9 November 2023

treated as solid in the model may have been hydrated in the real atmosphere, leading to an underestimation of $ALWC_{Inorg}$ hence overestimation of $ALWC_{OA}/ALWC$, as discussed in Jin et al. (2020).

In the flight region during the 2016 campaign, the RH was quite low, mostly below 40 %, with a median value of 38 %, and 25th and 75th percentiles of 24 % and 54 %, respectively. Within this RH range, the fraction of ALWC in total ambient aerosol mass is mostly below 10 % with at least 35 % of which contributed by OA-related ALW. In the 2018 campaign, flights primarily took place downwind of BB emissions, resulting in relatively high RHs, with the median values at 67 % and 25th and 75th percentiles at 55 % and 81 %, respectively. The majority of aerosols are with a fraction of $ALWC_{OA}$ in the total ALWC of around 37 %, and around 25 % of aerosols are with a $ALWC_{OA}$ contribution higher than 40 %. The mean contribution of $ALWC_{OA}$ to the total ALWC in both campaigns was around 38±16 %. Jin et al. (2020) reported a significant contribution of OA to ALWC obtained in Beijing (30±22 %), our result is even greater than this. It is similar to the 35 % obtained in Alabama forest and south-eastern US (Guo et al., 2015) and much higher than those in Carlton and Turpin (2013) and Hennigan et al. (2008), that suggested negligible contribution of OA to ALW.

3.3.3 Significance of κ_{OA} to ALWC over the SEA

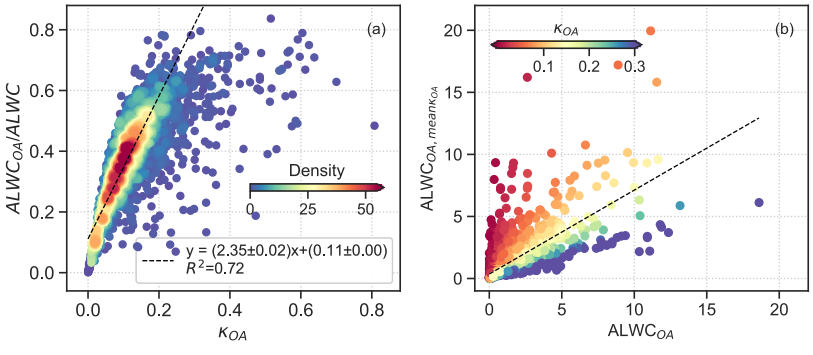

https://doi.org/10.5194/egusphere-2023-2319
Preprint. Discussion started: 9 November 2023

Figure 7. (a) Density plot of the variation of $ALWC_{OA}$/ALWC with κ_{OA}. (b) Comparison of $ALWC_{OA}$ calculated with real time retrieved κ_{OA} (x-axis) and the campaign mean value (i.e. 0.11±0.07) of κ_{OA} (y-axis), colored by κ_{OA}. The black dashed lines represent the linear fitting.

We further investigated the influencing factors of the $ALWC_{OA}$ contribution to ALWC. The RH and $ALWC_{OA}$ contribution show a very weak correlation, evidenced by the small variation of $ALWC_{OA}$/ALWC with RH (Fig. 6). The small variation of OA mass fraction (Fig. 2) also leads to a poor correlation between OA mass fraction and $ALWC_{OA}$/ALWC. However, κ_{OA} is found to be closely correlated with the $ALWC_{OA}$ contribution with an R^2 of 0.72 (Fig. 7). This good linear relationship between κ_{OA} and $ALWC_{OA}$/ALWC reveals the significant impact of OA hygroscopicity on ALWC over the SEA region during BB episode. The similar PDF distribution of κ_{OA} in both campaigns (Zhang et al., 2023) also explains the similar $ALWC_{OA}$ contribution (Fig. 2). Figure 7b further shows the comparison of $ALWC_{OA}$ calculated with retrieved (real-time) κ_{OA} and with its campaign average value (i.e. 0.11±0.08). The large discrepancy indicates the limitation of using a constant κ_{OA} for ALWC estimation as is usually done in most climate models (e.g. Ghan and Zaveri, 2007). A recent study indicated a small sensitivity of global climate forcing to κ_{OA}, varying it from 0.06 to 0.12 (Pöhlker et al., 2023). While this holds true for such small variation of κ_{OA}, in situations with larger κ_{OA} variations, as observed in this study, using a constant κ_{OA} can lead to large discrepancies. Our result highlights the importance of a good estimation of κ_{OA} and draws our attention to the variation of OA hygroscopicity in the SEA region, which is of great importance to the estimation of aerosol optical properties and CCN activation, thereby the aerosol direct radiative effect and cloud properties, both of which are critical for understanding regional climate processes and climate modeling.

4 Conclusion

https://doi.org/10.5194/egusphere-2023-2319
Preprint. Discussion started: 9 November 2023

The interaction between atmospheric aerosols and moisture is crucial for aerosol properties and their climate effects. In this study, we investigate the aerosol liquid water content (ALWC) and the fraction associated with organic aerosols (OA) over the south-eastern Atlantic Ocean during the BB season as part of the 2016 and 2018 ORACLES campaigns. The BBAs together with moisture coming from the fires in Africa are lifted to up to ~ 6 km and transported westwardly over the SEA. The 2016 ORACLES campaign performed around ~23° S-13° S was characterized by the African continent mid-level (~600 hPa) anticyclone, Benguela low-level jet, and subsidence off the coast of Namibian, encountering higher aerosol loading and lower RH, while the 2018 ORACLES campaign was more northerly with the southern African Easterly Jet as the most important characteristic, detecting lower aerosol loading and higher RH.

We calculated κ_{OA} following the ZSR mixing rule with $\kappa_{f(RH)}$, which was retrieved from Mie simulations with in-situ hygroscopicity measurement, size distribution, and chemical compositions assuming an internal mixing of particles. The mean κ_{OA} is 0.11±0.08, belonging to the upper median range reported in previous studies. The 5th, 25th, 75th, and 95th percentiles of κ_{OA} is 0.00, 0.06, 0.16, and 0.23, respectively. This large variation may be attributed to the substantial variations in the aging days of aerosols during transport. This study does not observe a clear correlation between κ_{OA} and the oxidation level of OA, a relationship often identified in previous studies, implying that factors beyond oxidation level plays a more vital role in OA hygroscopicity in this study.

The ALWC calculated from $\kappa_{f(RH)}$ ($ALWC_{\kappa_{f(RH)}}$) and as the sum of that for inorganics and for OA ($ALWC_{OA+ISRP}$) are compared in this study. Good agreement of ALWC from these two methods has been achieved for all RHs with an R^2 of 0.99. The vertical distribution of the mean and median values of ALWC are mostly smaller than 2.5 μg m^{-3}. ALWC increases with aerosol loading and ambient RH; the ALWC in 2016 is generally consistent with that in the

https://doi.org/10.5194/egusphere-2023-2319
Preprint. Discussion started: 9 November 2023

2018 campaign due to the lower RH and higher aerosol loading in the 2016 campaign, with the median ALWC being 1.6 μg m^{-3} and 1.4 μg m^{-3} in 2016 and 2018, respectively. These values are lower than those from the continent and even orders of magnitude smaller than in polluted regions.

The contribution of $ALWC_{OA}$ to the total ALWC was around 38±16 %. This high contribution of $ALWC_{OA}$ is greater than those commonly reported in the literature, highlighting the significant role of OA in ALWC in the SEA region during the BB season. OA mass fraction is weakly correlated to $ALWC_{OA}$/ALWC due to its limited variation; while $ALWC_{OA}$/ALWC and κ_{OA} are highly correlated (R^2=0.72). In addition, the $ALWC_{OA}$ calculated with real-time κ_{OA} and the campaign mean κ_{OA} differ substantially. These all demonstrate the importance of a good estimation of OA hygroscopicity, which is crucial to the aerosol direct radiative forcing and CCN activation in this climatically significant region, and imply the limitation of using a constant κ_{OA} value, as is commonly adopted by climate models.

Competing interests. At least one of the (co-)authors is a guest member of the editorial board of Atmospheric Chemistry and Physics for the special issue "New observations and related modelling studies of the aerosol-cloud-climate system in the Southeast Atlantic and southern Africa regions". The authors have no other competing interests to declare.

Data Availability. Data sets are publicly available via the digital object identifier provided under ORACLES Science Team reference: https://doi.org/10.5067/Suborbital/ORACLES/P3/2018_V2.

Acknowledgments. The authors would like to thank the ORACLES team. Lu Zhang thanks the postdoctoral fellowship funding from Tel Aviv University, Department of Exact Sciences. Michal Segal-Rozenhaimer and Haochi Che are supported by United States Department of

https://doi.org/10.5194/egusphere-2023-2319
Preprint. Discussion started: 9 November 2023

Energy Atmospheric System Research (ASR) grant DE-SC0020084. Caroline Dang thanks the NASA Postdoctoral Fellowship Grant. Paola Formenti is supported by the AErosols, RadiatiOn and CLOuds in southern Africa (AEROCLO-sA) project funded by the French National Research Agency under grant agreement n° ANR-15-CE01-0014-01, the French national programs LEFE/INSU and PNTS, the French National Agency for Space Studies (CNES), the European Union's 7th Framework Programme (FP7/2014-2018) under EUFAR2 contract n°312609, and the South African National Research Foundation (NRF) under grant UID 105958. The authors thank Paul Zieger for useful comments on this article.

Financial support. This research has been supported by the Tel Aviv University (postdoctoral fellowship); the United States Department of Energy (DOE) Atmospheric System Research (ASR; grant DE-SC0020084); a NASA postdoctoral fellowship; the AErosols, RadiatiOn and CLOuds in southern Africa (AEROCLO-sA) project funded by the French National Research Agency (grant agreement no. ANR-15-CE01-0014-01); the French national programs LEFE/INSU and PNTS; the French National Agency for Space Studies (CNES); the European Union's Seventh Framework Programme (FP7/2014-2018; EUFAR2 contract no. 312609); and the South African National Research Foundation (NRF; grant UID 105958).

References

Adebiyi, A. A. and Zuidema, P.: The role of the southern African easterly jet in modifying the southeast Atlantic aerosol and cloud environments, Q. J. R. Meteorol. Soc., 142, 1574–1589, https://doi.org/10.1002/qj.2765, 2016.

Adebiyi, A. A., Zuidema, P., and Abel, S. J.: The Convolution of Dynamics and Moisture with the Presence of Shortwave Absorbing Aerosols over the Southeast Atlantic, J. Clim., 28, 1997–2024, https://doi.org/10.1175/JCLI-D-14-00352.1, 2015.

Andela, N., Morton, D. C., Giglio, L., Chen, Y., van der Werf, G. R., Kasibhatla, P. S., DeFries, R. S., Collatz, G. J., Hantson, S., Kloster, S., Bachelet, D., Forrest, M., Lasslop, G., Li, F., Mangeon, S., Melton, J. R., Yue, C., and Randerson, J. T.: A human-driven decline in global burned area, Science, 356, 1356–1362, https://doi.org/10.1126/science.aal4108, 2017.

https://doi.org/10.5194/egusphere-2023-2319
Preprint. Discussion started: 9 November 2023

Bian, Y. X., Zhao, C. S., Ma, N., Chen, J., and Xu, W. Y.: A study of aerosol liquid water content based on hygroscopicity measurements at high relative humidity in the North China Plain, Atmospheric Chem. Phys., 14, 6417–6426, https://doi.org/10.5194/acp-14-6417-2014, 2014.

Bougiatioti, A., Nikolaou, P., Stavroulas, I., Kouvarakis, G., Weber, R., Nenes, A., Kanakidou, M., and Mihalopoulos, N.: Particle water and pH in the eastern Mediterranean: source variability and implications for nutrient availability, Atmospheric Chem. Phys., 16, 4579–4591, https://doi.org/10.5194/acp-16-4579-2016, 2016.

Burgos, M. A., Andrews, E., Titos, G., Alados-Arboledas, L., Baltensperger, U., Day, D., Jefferson, A., Kalivitis, N., Mihalopoulos, N., Sherman, J., Sun, J., Weingartner, E., and Zieger, P.: A global view on the effect of water uptake on aerosol particle light scattering, Sci. Data, 6, 157, https://doi.org/10.1038/s41597-019-0158-7, 2019.

Carlton, A. G. and Turpin, B. J.: Particle partitioning potential of organic compounds is highest in the Eastern US and driven by anthropogenic water, Atmospheric Chem. Phys., 13, 10203–10214, https://doi.org/10.5194/acp-13-10203-2013, 2013.

Cerully, K. M., Bougiatioti, A., Hite, J. R., Guo, H., Xu, L., Ng, N. L., Weber, R., and Nenes, A.: On the link between hygroscopicity, volatility, and oxidation state of ambient and water-soluble aerosols in the southeastern United States, Atmospheric Chem. Phys., 15, 8679–8694, https://doi.org/10.5194/acp-15-8679-2015, 2015.

Che, H., Segal-Rozenhaimer, M., Zhang, L., Dang, C., Zuidema, P., Dobracki, A., Sedlacek, A. J., Coe, H., Wu, H., Taylor, J., Zhang, X., Redemann, J., and Haywood, J.: Cloud processing and weeklong ageing affect biomass burning aerosol properties over the south-eastern Atlantic, Commun. Earth Environ., 3, 182, https://doi.org/10.1038/s43247-022-00517-3, 2022.

Che, H. C., Zhang, X. Y., Wang, Y. Q., Zhang, L., Shen, X. J., Zhang, Y. M., Ma, Q. L., Sun, J. Y., Zhang, Y. W., and Wang, T. T.: Characterization and parameterization of aerosol cloud condensation nuclei activation under different pollution conditions, Sci. Rep., 6, 24497, https://doi.org/10.1038/srep24497, 2016.

Dang, C., Segal-Rozenhaimer, M., Che, H., Zhang, L., Formenti, P., Taylor, J., Dobracki, A., Purdue, S., Wong, P.-S., Nenes, A., Sedlacek, A., Coe, H., Redemann, J., Zuidema, P., and Haywood, J.: Biomass burning and marine aerosol processing over the southeast Atlantic Ocean: A TEM single particle analysis, Atmospheric Chem. Phys. Discuss., 1–30, https://doi.org/10.5194/acp-2021-724, 2021.

Dang, C., Segal-Rozenhaimer, M., Che, H., Zhang, L., Formenti, P., Taylor, J., Dobracki, A., Purdue, S., Wong, P.-S., Nenes, A., Sedlacek III, A., Coe, H., Redemann, J., Zuidema, P., Howell, S., and Haywood, J.: Biomass burning and marine aerosol processing over the southeast Atlantic Ocean: a TEM single-particle analysis, Atmospheric Chem. Phys., 22, 9389–9412, https://doi.org/10.5194/acp-22-9389-2022, 2022.

Deng, Y., Yai, H., Fujinari, H., Kawana, K., Nakayama, T., and Mochida, M.: Diurnal variation and size dependence of the hygroscopicity of organic aerosol at a forest site in Wakayama, Japan: their relationship to CCN concentrations, Atmospheric Chem. Phys., 19, 5889–5903, https://doi.org/10.5194/acp-19-5889-2019, 2019.

https://doi.org/10.5194/egusphere-2023-2319
Preprint. Discussion started: 9 November 2023

Dobracki, A., Zuidema, P., Howell, S., Saide, P., Freitag, S., Aiken, A. C., Burton, S. P., Sedlacek III, A. J., Redemann, J., and Wood, R.: An attribution of the low single-scattering albedo of biomass-burning aerosol over the southeast Atlantic, Atmospheric Chem. Phys. Discuss., 1–40, https://doi.org/10.5194/acp-2022-501, 2022.

Engelhart, G. J., Moore, R. H., Nenes, A., and Pandis, S. N.: Cloud condensation nuclei activity of isoprene secondary organic aerosol, J. Geophys. Res. Atmospheres, 116, https://doi.org/10.1029/2010JD014706, 2011.

Fountoukis, C. and Nenes, A.: ISORROPIA II: a computationally efficient thermodynamic equilibrium model for K^+–Ca^{2+}–Mg^{2+}–NH_4^+–Na^+–$SO_4^{2−}$–$NO_3^{−}$ –$Cl^{−}$–H_2O aerosols, Atmospheric Chem. Phys., 7, 4639–4659, https://doi.org/10.5194/acp-7-4639-2007, 2007.

Ghan, S. J. and Zaveri, R. A.: Parameterization of optical properties for hydrated internally mixed aerosol, J. Geophys. Res. Atmospheres, 112, https://doi.org/10.1029/2006JD007927, 2007.

Guo, H., Xu, L., Bougiatioti, A., Cerully, K. M., Capps, S. L., Hite, J. R., Carlton, A. G., Lee, S.-H., Bergin, M. H., Ng, N. L., Nenes, A., and Weber, R. J.: Fine-particle water and pH in the southeastern United States, Atmospheric Chem. Phys., 15, 5211–5228, https://doi.org/10.5194/acp-15-5211-2015, 2015.

Hennigan, C. J., Bergin, M. H., Dibb, J. E., and Weber, R. J.: Enhanced secondary organic aerosol formation due to water uptake by fine particles, Geophys. Res. Lett., 35, https://doi.org/10.1029/2008GL035046, 2008.

Jin, X., Wang, Y., Li, Z., Zhang, F., Xu, W., Sun, Y., Fan, X., Chen, G., Wu, H., Ren, J., Wang, Q., and Cribb, M.: Significant contribution of organics to aerosol liquid water content in winter in Beijing, China, Atmospheric Chem. Phys., 20, 901–914, https://doi.org/10.5194/acp-20-901-2020, 2020.

Kuang, Y., Zhao, C. S., Zhao, G., Tao, J. C., Xu, W., Ma, N., and Bian, Y. X.: A novel method for calculating ambient aerosol liquid water content based on measurements of a humidified nephelometer system, Atmospheric Meas. Tech., 11, 2967–2982, https://doi.org/10.5194/amt-11-2967-2018, 2018.

Kuang, Y., Xu, W., Tao, J., Ma, N., Zhao, C., and Shao, M.: A Review on Laboratory Studies and Field Measurements of Atmospheric Organic Aerosol Hygroscopicity and Its Parameterization Based on Oxidation Levels, Curr. Pollut. Rep., 6, 410–424, https://doi.org/10.1007/s40726-020-00164-2, 2020a.

Kuang, Y., He, Y., Xu, W., Zhao, P., Cheng, Y., Zhao, G., Tao, J., Ma, N., Su, H., Zhang, Y., Sun, J., Cheng, P., Yang, W., Zhang, S., Wu, C., Sun, Y., and Zhao, C.: Distinct diurnal variation in organic aerosol hygroscopicity and its relationship with oxygenated organic aerosol, Atmospheric Chem. Phys., 20, 865–880, https://doi.org/10.5194/acp-20-865-2020, 2020b.

Kuang, Y., He, Y., Xu, W., Yuan, B., Zhang, G., Ma, Z., Wu, C., Wang, C., Wang, S., Zhang, S., Tao, J., Ma, N., Su, H., Cheng, Y., Shao, M., and Sun, Y.: Photochemical

https://doi.org/10.5194/egusphere-2023-2319
Preprint. Discussion started: 9 November 2023

553 Aqueous-Phase Reactions Induce Rapid Daytime Formation of Oxygenated Organic Aerosol
554 on the North China Plain, Environ. Sci. Technol., 54, 3849–3860,
555 https://doi.org/10.1021/acs.est.9b06836, 2020c.

556 Kuang, Y., Huang, S., Xue, B., Luo, B., Song, Q., Chen, W., Hu, W., Li, W., Zhao, P., Cai,
557 M., Peng, Y., Qi, J., Li, T., Wang, S., Chen, D., Yue, D., Yuan, B., and Shao, M.: Contrasting
558 effects of secondary organic aerosol formations on organic aerosol hygroscopicity,
559 Atmospheric Chem. Phys., 21, 10375–10391, https://doi.org/10.5194/acp-21-10375-2021,
560 2021.

561 Lambe, A. T., Onasch, T. B., Massoli, P., Croasdale, D. R., Wright, J. P., Ahern, A. T.,
562 Williams, L. R., Worsnop, D. R., Brune, W. H., and Davidovits, P.: Laboratory studies of the
563 chemical composition and cloud condensation nuclei (CCN) activity of secondary organic
564 aerosol (SOA) and oxidized primary organic aerosol (OPOA), Atmospheric Chem. Phys., 11,
565 8913–8928, https://doi.org/10.5194/acp-11-8913-2011, 2011.

566 Li, W., Teng, X., Chen, X., Liu, L., Xu, L., Zhang, J., Wang, Y., Zhang, Y., and Shi, Z.:
567 Organic Coating Reduces Hygroscopic Growth of Phase-Separated Aerosol Particles,
568 Environ. Sci. Technol., 55, 16339–16346, https://doi.org/10.1021/acs.est.1c05901, 2021.

569 Mei, F., Setyan, A., Zhang, Q., and Wang, J.: CCN activity of organic aerosols observed
570 downwind of urban emissions during CARES, Atmospheric Chem. Phys., 13, 12155–12169,
571 https://doi.org/10.5194/acp-13-12155-2013, 2013.

572 Milousis, A., Tsimpidi, A. P., Tost, H., Pandis, S. N., Nenes, A., Kiendler-Scharr, A., and
573 Karydis, V. A.: Implementation of the ISORROPIA-lite Aerosol Thermodynamics Model
574 into the EMAC Chemistry Climate Model 2.56: Implications for Aerosol Composition and
575 Acidity, Geosci. Model Dev. Discuss., 1–33, https://doi.org/10.5194/gmd-2023-178, 2023.

576 Nenes, A., Pandis, S. N., and Pilinis, C.: ISORROPIA: A New Thermodynamic Equilibrium
577 Model for Multiphase Multicomponent Inorganic Aerosols, Aquat. Geochem., 4, 123–152,
578 https://doi.org/10.1023/A:1009604003981, 1998.

579 Ng, N. L., Canagaratna, M. R., Jimenez, J. L., Chhabra, P. S., Seinfeld, J. H., and Worsnop,
580 D. R.: Changes in organic aerosol composition with aging inferred from aerosol mass spectra,
581 Atmospheric Chem. Phys., 11, 6465–6474, https://doi.org/10.5194/acp-11-6465-2011, 2011.

582 Nicholson, S. E.: A low-level jet along the Benguela coast, an integral part of the Benguela
583 current ecosystem, Clim. Change, 99, 613–624, https://doi.org/10.1007/s10584-009-9678-z,
584 2010.

585 Peng, C., Chen, L., and Tang, M.: A database for deliquescence and efflorescence relative
586 humidities of compounds with atmospheric relevance, Fundam. Res., 2, 578–587,
587 https://doi.org/10.1016/j.fmre.2021.11.021, 2022.

588 Petters, M. D. and Kreidenweis, S. M.: A single parameter representation of hygroscopic
589 growth and cloud condensation nucleus activity, Atmos Chem Phys, 11, 2007.

590 Petters, M. D., Carrico, C. M., Kreidenweis, S. M., Prenni, A. J., DeMott, P. J., Collett, J. L.,
591 and Moosmüller, H.: Cloud condensation nucleation activity of biomass burning aerosol, J.
592 Geophys. Res., 114, D22205, https://doi.org/10.1029/2009JD012353, 2009.

https://doi.org/10.5194/egusphere-2023-2319
Preprint. Discussion started: 9 November 2023

593 Pilinis, C., Spyros N., P., and John H., S.: Sensitivity of direct climate forcing by atmospheric
594 aerosols to aerosol size and composition, J. Geophys. Res. Atmospheres, 100, 18739–18754,
595 https://doi.org/10.1029/95JD02119, 1995.

596 Pistone, K., Zuidema, P., Wood, R., Diamond, M., da Silva, A. M., Ferrada, G., Saide, P. E.,
597 Ueyama, R., Ryoo, J.-M., Pfister, L., Podolske, J., Noone, D., Bennett, R., Stith, E.,
598 Carmichael, G., Redemann, J., Flynn, C., LeBlanc, S., Segal-Rozenhaimer, M., and
599 Shinozuka, Y.: Exploring the elevated water vapor signal associated with the free
600 tropospheric biomass burning plume over the southeast Atlantic Ocean, Atmospheric Chem.
601 Phys., 21, 9643–9668, https://doi.org/10.5194/acp-21-9643-2021, 2021.

602 Pöhlker, M. L., Pöhlker, C., Quaas, J., Mülmenstädt, J., Pozzer, A., Andreae, M. O., Artaxo,
603 P., Block, K., Coe, H., Ervens, B., Gallimore, P., Gaston, C. J., Gunthe, S. S., Henning, S.,
604 Herrmann, H., Krüger, O. O., McFiggans, G., Poulain, L., Raj, S. S., Reyes-Villegas, E.,
605 Royer, H. M., Walter, D., Wang, Y., and Pöschl, U.: Global organic and inorganic aerosol
606 hygroscopicity and its effect on radiative forcing, Nat. Commun., 14, 6139,
607 https://doi.org/10.1038/s41467-023-41695-8, 2023.

608 Rastak, N., Pajunoja, A., Acosta Navarro, J. C., Ma, J., Song, M., Partridge, D. G., Kirkevåg,
609 A., Leong, Y., Hu, W. W., Taylor, N. F., Lambe, A., Cerully, K., Bougiatioti, A., Liu, P.,
610 Krejci, R., Petäjä, T., Percival, C., Davidovits, P., Worsnop, D. R., Ekman, A. M. L., Nenes,
611 A., Martin, S., Jimenez, J. L., Collins, D. R., Topping, D. o., Bertram, A. K., Zuend, A.,
612 Virtanen, A., and Riipinen, I.: Microphysical explanation of the RH-dependent water affinity
613 of biogenic organic aerosol and its importance for climate, Geophys. Res. Lett., 44, 5167–
614 5177, https://doi.org/10.1002/2017GL073056, 2017.

615 Redemann, J., Wood, R., Zuidema, P., Doherty, S. J., Luna, B., LeBlanc, S. E., Diamond, M.
616 S., Shinozuka, Y., Chang, I. Y., Ueyama, R., Pfister, L., Ryoo, J.-M., Dobracki, A. N., da
617 Silva, A. M., Longo, K. M., Kacenelenbogen, M. S., Flynn, C. J., Pistone, K., Knox, N. M.,
618 Piketh, S. J., Haywood, J. M., Formenti, P., Mallet, M., Stier, P., Ackerman, A. S., Bauer, S.
619 E., Fridlind, A. M., Carmichael, G. R., Saide, P. E., Ferrada, G. A., Howell, S. G., Freitag, S.,
620 Cairns, B., Holben, B. N., Knobelspiesse, K. D., Tanelli, S., L'Ecuyer, T. S., Dzambo, A. M.,
621 Sy, O. O., McFarquhar, G. M., Poellot, M. R., Gupta, S., O'Brien, J. R., Nenes, A., Kacarab,
622 M., Wong, J. P. S., Small-Griswold, J. D., Thornhill, K. L., Noone, D., Podolske, J. R.,
623 Schmidt, K. S., Pilewskie, P., Chen, H., Cochrane, S. P., Sedlacek, A. J., Lang, T. J., Stith,
624 E., Segal-Rozenhaimer, M., Ferrare, R. A., Burton, S. P., Hostetler, C. A., Diner, D. J.,
625 Seidel, F. C., Platnick, S. E., Myers, J. S., Meyer, K. G., Spangenberg, D. A., Maring, H., and
626 Gao, L.: An overview of the ORACLES (ObseRvations of Aerosols above CLouds and their
627 intEractionS) project: aerosol–cloud–radiation interactions in the southeast Atlantic basin,
628 Atmospheric Chem. Phys., 21, 1507–1563, https://doi.org/10.5194/acp-21-1507-2021, 2021.

629 Ren, J., Tan, W., Tian, X., Wu, Z., Li, C., Li, J., Zhao, C., Liu, D., Kang, L., and Zhu, T.:
630 Retrieval of aerosol liquid water content from high spectral resolution lidar, Sci. Total
631 Environ., 799, 149423, https://doi.org/10.1016/j.scitotenv.2021.149423, 2021.

632 Rickards, A. M. J., Miles, R. E. H., Davies, J. F., Marshall, F. H., and Reid, J. P.:
633 Measurements of the Sensitivity of Aerosol Hygroscopicity and the κ Parameter to the O/C
634 Ratio, J. Phys. Chem. A, 117, 14120–14131, https://doi.org/10.1021/jp407991n, 2013.

635 Ryoo, J.-M., Pfister, L., Ueyama, R., Zuidema, P., Wood, R., Chang, I., and Redemann, J.: A
636 meteorological overview of the ORACLES (ObseRvations of Aerosols above CLouds and

https://doi.org/10.5194/egusphere-2023-2319
Preprint. Discussion started: 9 November 2023

their intEractionS) campaign over the southeastern Atlantic during 2016–2018: Part 1 – Climatology, Atmospheric Chem. Phys., 21, 16689–16707, https://doi.org/10.5194/acp-21-16689-2021, 2021.

Schill, G. P., Froyd, K. D., Bian, H., Kupc, A., Williamson, C., Brock, C. A., Ray, E., Hornbrook, R. S., Hills, A. J., Apel, E. C., Chin, M., Colarco, P. R., and Murphy, D. M.: Widespread biomass burning smoke throughout the remote troposphere, Nat. Geosci., 13, 422–427, https://doi.org/10.1038/s41561-020-0586-1, 2020.

Song, S., Gao, M., Xu, W., Sun, Y., Worsnop, D. R., Jayne, J. T., Zhang, Y., Zhu, L., Li, M., Zhou, Z., Cheng, C., Lv, Y., Wang, Y., Peng, W., Xu, X., Lin, N., Wang, Y., Wang, S., Munger, J. W., Jacob, D. J., and McElroy, M. B.: Possible heterogeneous chemistry of hydroxymethanesulfonate (HMS) in northern China winter haze, Atmospheric Chem. Phys., 19, 1357–1371, https://doi.org/10.5194/acp-19-1357-2019, 2019.

Thompson, G. and Eidhammer, T.: A Study of Aerosol Impacts on Clouds and Precipitation Development in a Large Winter Cyclone, J. Atmospheric Sci., 71, 3636–3658, https://doi.org/10.1175/JAS-D-13-0305.1, 2014.

Titos, G., Cazorla, A., Zieger, P., Andrews, E., Lyamani, H., Granados-Muñoz, M. J., Olmo, F. J., and Alados-Arboledas, L.: Effect of hygroscopic growth on the aerosol light-scattering coefficient: A review of measurements, techniques and error sources, Atmos. Environ., 141, 494–507, https://doi.org/10.1016/j.atmosenv.2016.07.021, 2016.

Wang, G., Zhang, R., Gomez, M. E., Yang, L., Levy Zamora, M., Hu, M., Lin, Y., Peng, J., Guo, S., Meng, J., Li, J., Cheng, C., Hu, T., Ren, Y., Wang, Y., Gao, J., Cao, J., An, Z., Zhou, W., Li, G., Wang, J., Tian, P., Marrero-Ortiz, W., Secrest, J., Du, Z., Zheng, J., Shang, D., Zeng, L., Shao, M., Wang, W., Huang, Y., Wang, Y., Zhu, Y., Li, Y., Hu, J., Pan, B., Cai, L., Cheng, Y., Ji, Y., Zhang, F., Rosenfeld, D., Liss, P. S., Duce, R. A., Kolb, C. E., and Molina, M. J.: Persistent sulfate formation from London Fog to Chinese haze, Proc. Natl. Acad. Sci., 113, 13630–13635, https://doi.org/10.1073/pnas.1616540113, 2016.

van der Werf, G. R., Randerson, J. T., Giglio, L., Collatz, G. J., Mu, M., Kasibhatla, P. S., Morton, D. C., DeFries, R. S., Jin, Y., and van Leeuwen, T. T.: Global fire emissions and the contribution of deforestation, savanna, forest, agricultural, and peat fires (1997–2009), Atmospheric Chem. Phys., 10, 11707–11735, https://doi.org/10.5194/acp-10-11707-2010, 2010.

Wexler, A. S. and Clegg, S. L.: Atmospheric aerosol models for systems including the ions H+, NH4+, Na+, SO42−, NO3−, Cl−, Br−, and H2O, J. Geophys. Res. Atmospheres, 107, ACH 14-1-ACH 14-14, https://doi.org/10.1029/2001JD000451, 2002.

WMO/GAW, W. M.: GAW Report, 227. WMO/GAW Aerosol Measurement Procedures, Guidelines and Recommendations, 2nd edition., WMO, Geneva, 103 p. pp., 2016.

Wu, H., Taylor, J. W., Szpek, K., Langridge, J. M., Williams, P. I., Flynn, M., Allan, J. D., Abel, S. J., Pitt, J., Cotterell, M. I., Fox, C., Davies, N. W., Haywood, J., and Coe, H.: Vertical variability of the properties of highly aged biomass burning aerosol transported over the southeast Atlantic during CLARIFY-2017, Atmospheric Chem. Phys., 20, 12697–12719, https://doi.org/10.5194/acp-20-12697-2020, 2020.

https://doi.org/10.5194/egusphere-2023-2319
Preprint. Discussion started: 9 November 2023

678 Zhang, L., Sun, J. Y., Shen, X. J., Zhang, Y. M., Che, H., Ma, Q. L., Zhang, Y. W., Zhang, X.
679 Y., and Ogren, J. A.: Observations of relative humidity effects on aerosol light scattering in
680 the Yangtze River Delta of China, Atmospheric Chem. Phys., 15, 8439–8454,
681 https://doi.org/10.5194/acp-15-8439-2015, 2015.

682 Zhang, L., Segal-Rozenhaimer, M., Che, H., Dang, C., Sedlacek III, A. J., Lewis, E. R.,
683 Dobracki, A., Wong, J. P. S., Formenti, P., Howell, S. G., and Nenes, A.: Light Absorption
684 by Brown Carbon over the South-East Atlantic Ocean, https://doi.org/10.5194/acp-2021-
685 1000, 2022.

686 Zhang, L., Segal-Rozenhaimer, M., Che, H., Dang, C., Sun, J., Kuang, Y., Formenti, P., and
687 Howell, S.: Aerosol hygroscopicity over the South-East Atlantic Ocean during the biomass
688 burning season: Part I − From the perspective of scattering enhancement, EGUsphere, 1–34,
689 https://doi.org/10.5194/egusphere-2023-2199, 2023.

690 Zhang, Q., Jimenez, J. L., Canagaratna, M. R., Allan, J. D., Coe, H., Ulbrich, I., Alfarra, M.
691 R., Takami, A., Middlebrook, A. M., Sun, Y. L., Dzepina, K., Dunlea, E., Docherty, K.,
692 DeCarlo, P. F., Salcedo, D., Onasch, T., Jayne, J. T., Miyoshi, T., Shimono, A., Hatakeyama,
693 S., Takegawa, N., Kondo, Y., Schneider, J., Drewnick, F., Borrmann, S., Weimer, S.,
694 Demerjian, K., Williams, P., Bower, K., Bahreini, R., Cottrell, L., Griffin, R. J., Rautiainen,
695 J., Sun, J. Y., Zhang, Y. M., and Worsnop, D. R.: Ubiquity and dominance of oxygenated
696 species in organic aerosols in anthropogenically-influenced Northern Hemisphere
697 midlatitudes, Geophys. Res. Lett., 34, https://doi.org/10.1029/2007GL029979, 2007.

698 Zieger, P., Fierz-Schmidhauser, R., Gysel, M., Ström, J., Henne, S., Yttri, K. E.,
699 Baltensperger, U., and Weingartner, E.: Effects of relative humidity on aerosol light
700 scattering in the Arctic, Atmospheric Chem. Phys., 10, 3875–3890,
701 https://doi.org/10.5194/acp-10-3875-2010, 2010.

702 Zieger, P., Fierz-Schmidhauser, R., Weingartner, E., and Baltensperger, U.: Effects of
703 relative humidity on aerosol light scattering: results from different European sites,
704 Atmospheric Chem. Phys., 13, 10609–10631, https://doi.org/10.5194/acp-13-10609-2013,
705 2013.

706